

N66 24611

5. COMPARISON OF WIND-TUNNEL AND FLIGHT RESULTS ON  
A FOUR-PROPELLER TILT-WING CONFIGURATION

By Kenneth W. Goodson

NASA Langley Research Center

SUMMARY

24611

Over the years aerodynamicists have learned to rely heavily on wind-tunnel-model results in predicting the aerodynamic characteristics of conventional aircraft configurations. With the development of V/STOL configurations which have high slipstream deflection angles, such as the four-propeller tilt-wing XC-142A V/STOL aircraft, the reliability of small-scale wind-tunnel-model results in predicting full-scale airplane characteristics needs to be reexamined.

Extensive tests have been made by NASA on several sizes of wind-tunnel models of the XC-142A V/STOL configuration and by Ling-Temco-Vought, Inc., on the airplane. These results show that models predict the slow-speed level-flight characteristics very well but that small models underpredict the descent capability of the airplane. Larger scale wind-tunnel models of approximately half size show better agreement with the airplane descent characteristics.



5

It was found from smoke flow studies that small models can also predict the region in which self-generated disturbances will be encountered by tilt-wing configurations in ground proximity.

INTRODUCTION

Author

Over the years aerodynamists and designers have learned to rely heavily on model results in predicting the aerodynamic characteristics of conventional aircraft configurations; of course, appropriate corrections had to be applied to account for Reynolds number, Mach number, and tunnel wall effects. With the trend toward powered-lift configurations, the question naturally arises as to how reliable are small-scale-model results in predicting full-scale characteristics. Some early experience with the VZ-2 tilt-wing configuration (refs. 1 to 4) showed that model results predicted the level-flight characteristics reasonably well. (See ref. 5.)

This early work on tilt-wing configurations culminated in the design of the XC-142A V/STOL transport aircraft. NASA has conducted extensive wind-tunnel programs on the XC-142A configuration. (See refs. 6 to 8.) Two of the models used in these programs are shown in figure 1. Figure 1(a)

shows the 0.09-scale model used in the 17-foot test section of the Langley 300-MPH 7- by 10-foot tunnel, and figure 1(b) shows the 0.60-scale model used in the Ames 40- by 80-foot tunnel.

#### SYMBOLS

A	propeller disk area, $\text{ft}^2$
$C_D$	drag coefficient
$C_L$	lift coefficient
D	propeller diameter, ft
h	fuselage-bottom height from ground, ft
$h_R$	flow recirculation height, ft
$h/D$	ratio of fuselage height to propeller diameter
$i_w$	wing incidence angle with respect to fuselage, deg
q	free-stream dynamic pressure
$\dot{r}_{\text{MAX}}$	maximum self-generated yaw acceleration, $\text{deg}/\text{sec}^2$
S	wing area, $\text{ft}^2$
T	airplane thrust required, lb
$T/A$	propeller disk loading, $\text{lb}/\text{ft}^2$
V	velocity, knots
W	airplane weight, lb
$W/S$	wing loading, $\text{lb}/\text{ft}^2$
x	distance recirculating flow is projected in front of wing pivot, ft
$x/D$	ratio of forward projection of recirculating flow to propeller diameter
$\beta_{.75R}$	propeller blade angle at 0.75-radius station, deg
$\gamma$	flight-path angle, $\tan^{-1}(C_D/C_L)$ , deg
$\delta_f$	flap deflection angle, deg

## DISCUSSION

### Level Flight Transition

The wing tilt angles required in a steady-level flight transition for a wing loading of  $70 \text{ lb/ft}^2$  are shown in figure 2. For this comparison the fuselage was held level and the design landing-flap program was used. In general, the model results bracket the scatter band of the flight-test data with the small-scale-model data slightly underpredicting and the large-scale-model data slightly overpredicting the wing incidence angle required. Figure 3 shows the thrust required in transition and indicates good agreement between the models and airplane.

The model data have been limited to velocities above that for which flow breakdown occurs in wind tunnels for models with large wake deflection angles. These limitations have been found by William H. Rae, Jr., of the University of Washington and are discussed in paper no. 24 by Harry H. Heyson and Kalman J. Grunwald.

Figures 2 and 3 show, as did similar previous data on the VZ-2 tilt-wing airplane (ref. 5), that level flight characteristics can be predicted very well from model force data.

### Descent Limitations

The problem of determining descent limitations from wind-tunnel tests is one of determining what parameters can be measured in wind-tunnel tests that will make it possible to predict the limiting rate of descent of an airplane. The maximum rate of descent of a tilt-wing V/STOL airplane is limited by flow separation on the wings. The flow separation is manifested to the pilot as buffet and a deterioration in handling qualities. In both the buffet and the handling qualities, a pilot judgment is required in order to determine the airplane descent limitations. Neither of these characteristics, however, can be measured directly in wind-tunnel tests. For free-flight tunnel models, a pilot judgment is also required. Here the pilots, who fly the model remotely, determine the descent conditions and assign ratings to the model handling qualities by using a system similar to the Cooper airplane rating system. With force test models other techniques must be used. For the results reported in this paper tuft studies were used to indicate the angle of attack at which wing stall first occurs, along with the accompanying lift and drag.

Free-flight models.- Figure 4 compares the descent boundaries predicted by observing the flying characteristics of an 0.11-scale free-flight model with those observed on the airplane. The solid curves for the airplane indicate buffet onset at a descent angle of about  $-10^\circ$ ; as the airplane rate of descent was increased, the buffet increased and the handling qualities deteriorated to the point that flight was limited to a descent angle of about  $-15^\circ$ . Now if the airplane boundaries are compared with the free-flight-model boundaries, it can be seen that initial disturbances with the model occurred at a

descent angle of about  $-6^\circ$  and the flying characteristics became unacceptable at about  $-10^\circ$ . It is believed that this difference between the airplane and the small-model results is primarily due to the lower Reynolds number of the model tests.

Force-test models.- As indicated in paper no. 4 by James L. Hassell and Robert H. Kirby, buffet and deterioration of handling qualities would not be expected to occur until after the breakdown of flow on the wing; therefore, tufts are used on force models to indicate the angle of attack at which local wing stall (see fig. 5) is first encountered. The limiting descent angles are then determined from the lift and drag force data at these angles of attack.

The descent boundaries determined by this technique are shown in figure 6. The descent angles determined from flow studies and force data (corrected for wall effects) of the 0.60-scale model fall between the boundaries obtained with the airplane. For a wing incidence angle of  $20^\circ$ , the model results indicate a descent angle of about  $-14^\circ$ . These same results when uncorrected for wall effects gave a descent angle of about  $-12^\circ$ . Wall corrections would be greater for larger wing incidence angles and would become inadequate for extremely large wake deflection angles, depending upon tunnel/model size. The data for the small 0.09-scale model (uncorrected for wall effects) considerably underpredict the airplane values. Note that the 0.09-scale-model data give results very similar to those previously shown for the small-scale free-flight model. (Compare figs. 4 and 6.) Again it is believed that this underprediction by the small model is primarily the result of low slipstream Reynolds number.

Recently data have also been obtained which show that propeller blade angle can have considerable effect on the estimated descent angles. (See fig. 7 and ref. 7.) Figure 7 shows that, for both the small 0.09-scale model and the larger 0.60-scale model, reducing the propeller blade angle increases the estimated descent angle. This shows that propeller blade angle and possibly other propeller characteristics should be simulated in model tests if the airplane descent angles are to be simulated.

#### Self-Induced Turbulence in Ground Proximity

A problem of current interest with many V/STOL configurations is self-generated disturbances encountered in ground effect. In general, an airplane supports itself by deflecting air downward. In the transition speed range, the downward deflection of the air approaches the vertical as the speed approaches zero. When the airplane approaches the ground (see the sketch at the right of fig. 8), the downward flow is stopped by the ground and, at sufficiently low airplane speeds, some of it is deflected forward ahead of the airplane and creates a turbulent region within which the airplane must fly. Within the turbulent region the present tilt-wing airplane experiences large yaw accelerations. At the left of the figure is plotted the yaw acceleration in  $\text{deg}/\text{sec}^2$  against wing incidence angles in degrees. These results were obtained for the landing-flap program of the airplane. This figure shows that the airplane experiences large disturbances (of the same order as the hovering control available) for wing incidence angles between  $30^\circ$  and  $80^\circ$ . This range

corresponds to velocities from 30 knots down to about 12 knots. For speeds above 30 knots ( $i_w$  less than  $30^\circ$ ) no disturbances were encountered. At these higher speeds the slipstream was not projected ahead of the airplane.

The recirculating flow which causes these disturbances has also been observed in wind-tunnel tests with the 0.09-scale model. In figure 9 the height, in terms of propeller diameters, at which recirculation is first detected is plotted against a speed parameter which is the ratio of operating disk loading to free-stream dynamic pressure. Increasing values of this parameter represent decreasing speed. These results were obtained for a series of wing incidence angles by lowering the model toward the ground until the beginning of recirculation of the flow was observed. Note the correlation of these data with the faired straight line. These data indicate that the height at which a disturbance is first encountered increases with decreasing speed. It should be mentioned here that, for  $i_w = 45^\circ$ , the smoke studies showed that out of ground effect the slipstream tended to move outboard toward the wing tip and be swept downstream. As the height was reduced to 1 or 2 diameters, the flow fluctuated from inboard to outboard, being very erratic; as the height was further reduced to about 0.5 diameter, the flow moved inboard and toward the fuselage nose, still being very erratic. At a lower height (approximately landing-gear height) the flow became more steady. These results were obtained by using the moving endless-belt ground plane discussed in paper no. 25 by Thomas R. Turner.

The heights and velocities as predicted from this model curve (fig. 9) are compared in figure 10 with data obtained with the airplane. Here the height in feet is plotted against velocity in knots. The dashed line presents the data from figure 9 for the 0.09-scale model with flaps deflected  $60^\circ$ . The shaded area is based on disturbances observed by the pilot of the airplane. The difference between these curves is that the dashed curve represents the very onset of recirculation (based on smoke flows) whereas the shaded area represents the condition for which recirculation disturbances had developed sufficiently to be noticeable to the pilot.

The development of the disturbed region can also be measured in terms of the forward projection of the flow as shown in figure 11. Here the forward projection of the flow in propeller diameters (as defined by the sketch at the right of the figure) is shown as a function of wing incidence angle. These data are from model tests at a height of 0.5 diameter. The initial indications of recirculation with the model were observed for a wing incidence of about  $30^\circ$  (the end of the solid line). As the wing incidence was increased, the forward projection of the flow disturbance increased and exceeded 3 diameters for the wing incidence of  $45^\circ$ . The extent of the disturbance was also studied recently with the airplane. Airplane flights were made in a smoke flow field generated by ejecting oil into the engine exhaust. Initial indications of recirculation (smoke flow) for the airplane were also observed at a wing incidence of about  $30^\circ$ , which is in good agreement with the model results. The disturbances were not felt by the pilot, however, until the forward edge of the disturbed region reached the fuselage nose - a forward projection of about 1.5 diameters, as indicated by the circular symbol on the curve. This result is also in good agreement with the model results.

## CONCLUDING REMARKS

It should be noted that model results obtained on the tilt-wing XC-142A aircraft configuration, as well as results obtained from previous tests of the VZ-2 tilt-wing configuration, have shown that:

Level-flight-transition performance characteristics can be adequately predicted by using scale models. The small-scale-model results, however, are conservative in predicting the descent capability, since the actual airplane could achieve higher descent angles. Larger scale models of approximately half size are in better agreement with airplane descent characteristics.

The flow recirculation results presented show that small-size models can predict the conditions under which self-generated disturbances in ground effect will be encountered.

## REFERENCES

1. Pegg, Robert J.: Summary of Flight-Test Results of the VZ-2 Tilt-Wing Aircraft. NASA TN D-989, 1962.
2. Mitchell, Robert G.: Full-Scale Wind-Tunnel Test of the VZ-2 VTOL Airplane With Particular Reference to the Wing Stall Phenomena. NASA TN D-2013, 1963.
3. Schade, Robert O.; and Kirby, Robert H.: Effect of Wing Stalling in Transition on a 1/4-Scale Model of the VZ-2 Aircraft. NASA TN D-2381, 1964.
4. Kirby, Robert H.; Schade, Robert O.; and Tosti, Louis P.: Force-Test Investigation of a 1/4-Scale Model of the Modified VZ-2 Aircraft. NASA TN D-2382, 1964.
5. Staff of Powered-Lift Aerodynamics Section, NASA Langley Res. Center: Wall Effects and Scale Effects in V/STOL Model Testing. AIAA Aerodynamic Testing Conf., Mar. 1964, pp. 8-16.
6. Newsom, William A., Jr.; and Kirby, Robert H.: Flight Investigation of Stability and Control Characteristics of a 1/9-Scale Model of a Four-Propeller Tilt-Wing V/STOL Transport. NASA TN D-2443, 1964.
7. Goodson, Kenneth W.: Longitudinal Aerodynamic Characteristics of a Flapped Tilt-Wing Four-Propeller V/STOL Transport Model. NASA TN D-3217, 1966.
8. Deckert, Wallace H.; Page, V. Robert; and Dickinson, Stanley O.: Large-Scale Wind-Tunnel Tests of Descent Performance of an Airplane Model With a Tilt Wing and Differential Propeller Thrust. NASA TN D-1857, 1964.

0.09 - SCALE MODEL OF XC-142A

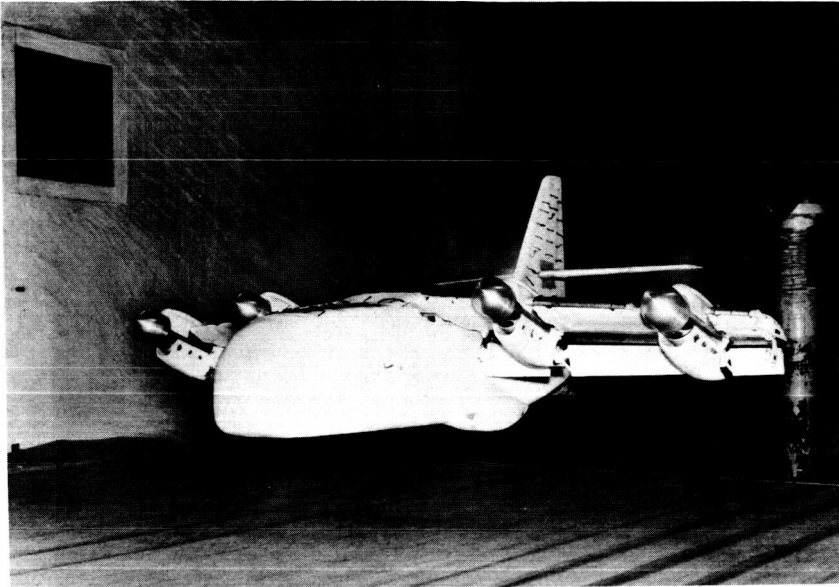


Figure 1(a)

L-2646-1

0.60 - SCALE MODEL OF XC-142A

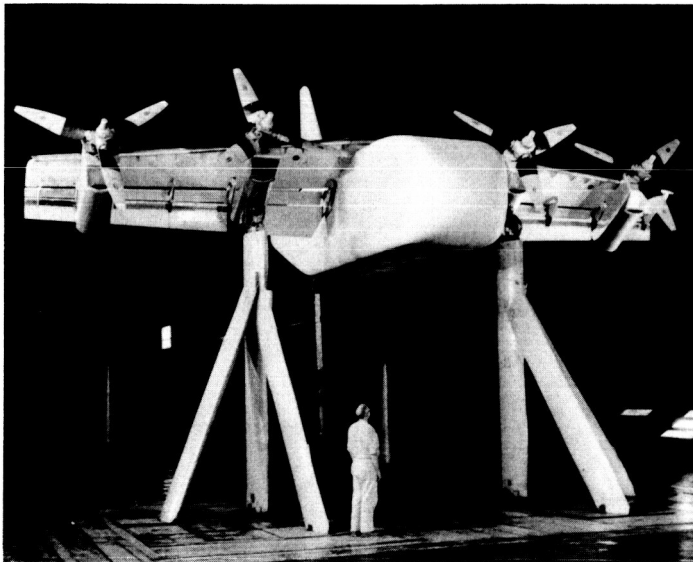


Figure 1(b)

L-2646-2

WING INCIDENCE REQUIRED IN LEVEL FLIGHT  
 $W/S = 70 \text{ LB/FT}^2$

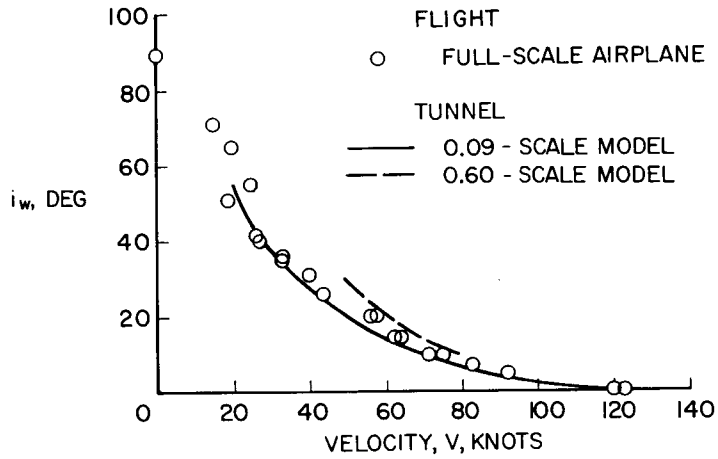


Figure 2

THRUST REQUIRED IN LEVEL FLIGHT  
 $W/S = 70 \text{ LB/FT}^2$

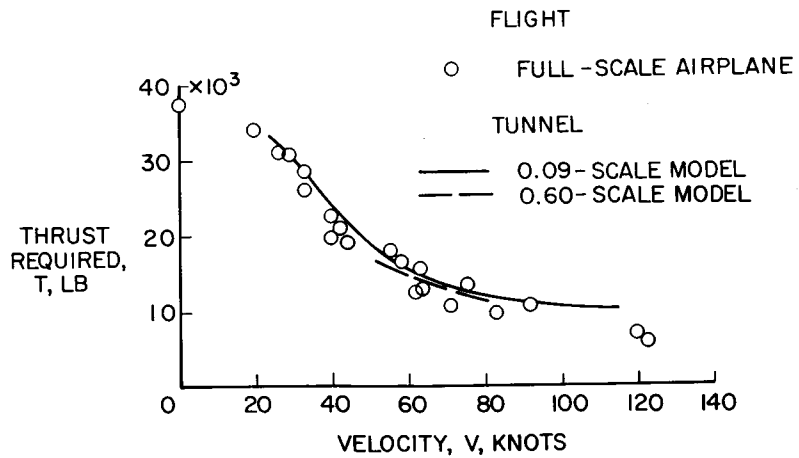


Figure 3



## DESCENT BOUNDARIES FOR FREE-FLIGHT MODEL

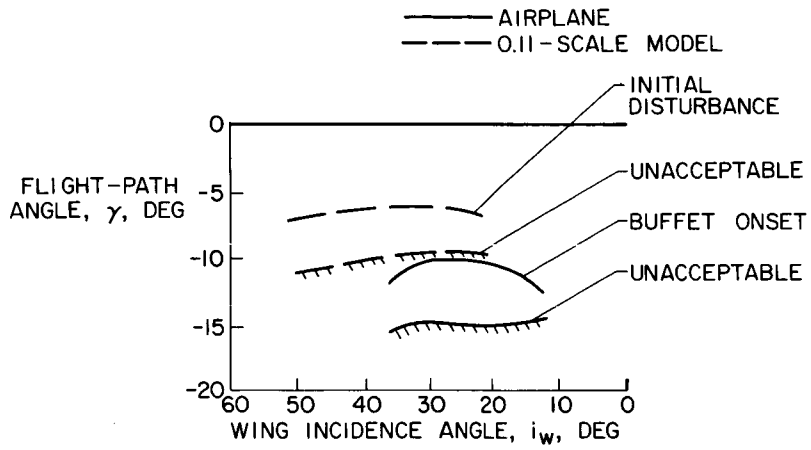


Figure 4

## INITIAL WING STALL FROM TUFT STUDIES

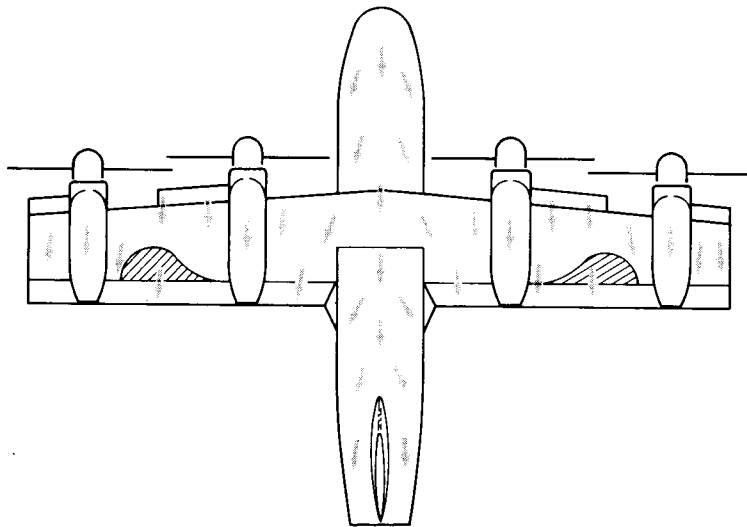


Figure 5

## DESCENT BOUNDARIES FROM TUFT STUDIES

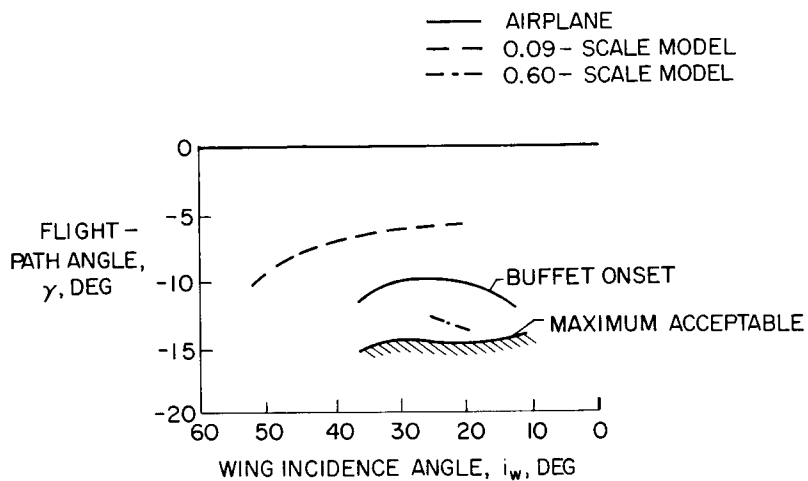


Figure 6

## EFFECT OF PROPELLER BLADE ANGLE

$i_w = 20^\circ; \delta_f = 60^\circ; W/S = 70 \text{ LB/FT}^2$

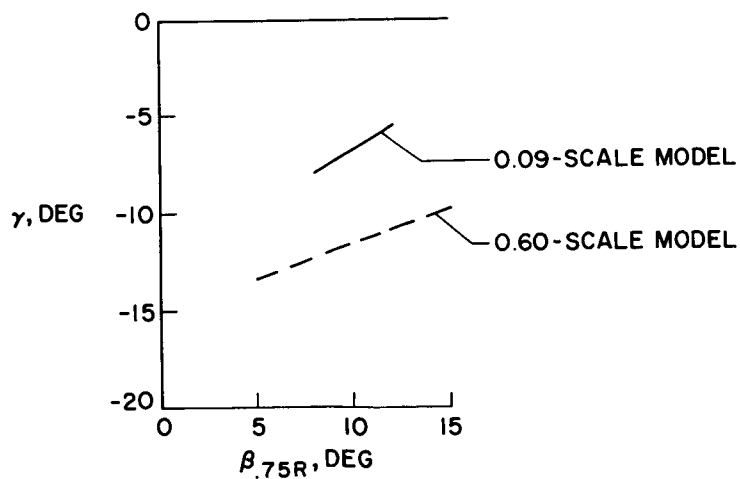


Figure 7

## EFFECT OF GROUND ON YAW ACCELERATIONS

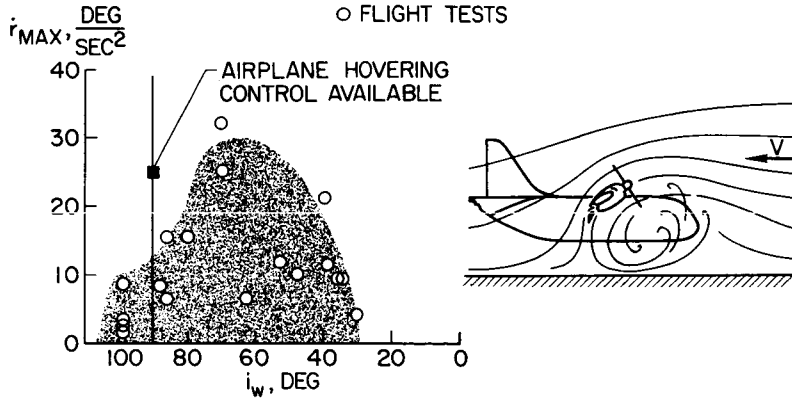


Figure 8

## VARIATION OF RECIRCULATION HEIGHT WITH RATIO OF DISK LOADING TO DYNAMIC PRESSURE $\delta_f = 60^\circ$

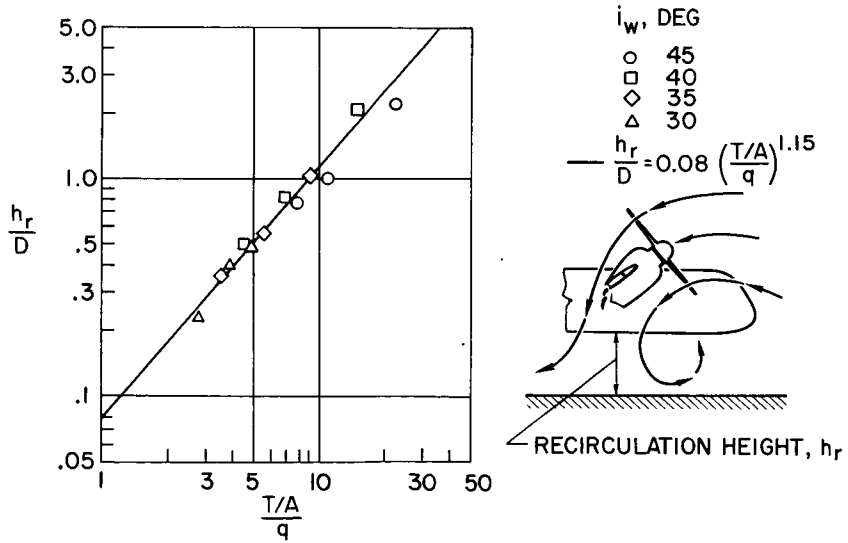


Figure 9

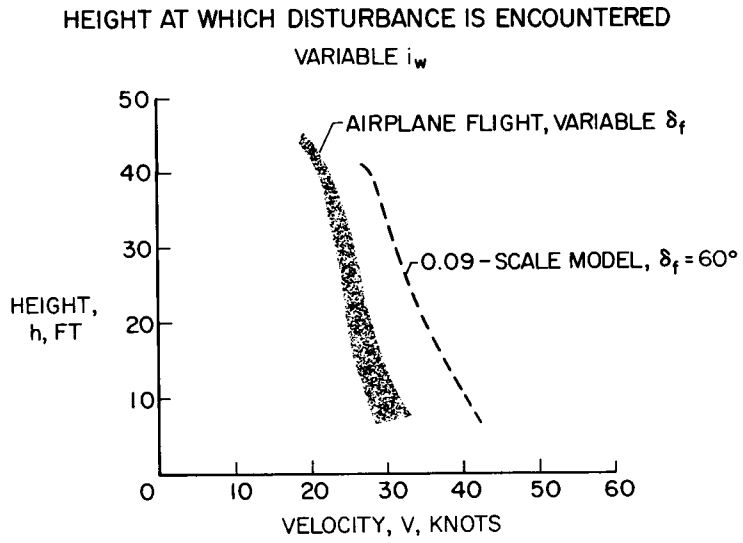


Figure 10

FORWARD EXTENT OF DISTURBED FLOW REGION  
 $\delta_f = 60^\circ$ ;  $h/D = 0.5$

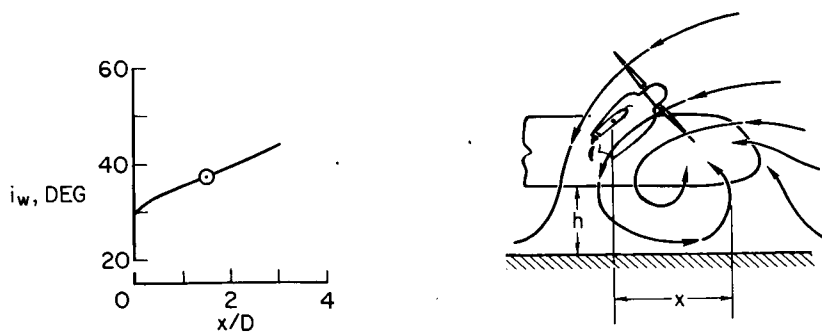


Figure 11